Pergamon

Cement and Concrete Research, Vol. 28, No. 3, pp. 401–410, 1998

0008-8846/98 $19.00 + .00

PII S0008-8846(97)00263-9

MICROSTRUCTURAL INVESTIGATION OF SEVERE DISTRESS IN A CRUSHED CONCRETE BASE

S.L. Sarkar[1]* and D.N. Little†
*Sarkar & Associates, Inc., 2501 Central Parkway, Houston, Texas 77092 USA
†Texas Transportation Institute, Texas A&M University, College Station, Texas 77843 USA

(Received April 16, 1997; in final form December 1, 1997)

ABSTRACT

A large parking lot was constructed on a crushed concrete base overlying a lime-stabilized subgrade. Despite adequate thickness of the subgrade and base, and having followed the construction codes and engineering specifications, within a very short period of time the base developed severe distress in the form of massive heaving and rutting. Microstructural investigation revealed intense sulfate attack, resulting from contamination of the crushed concrete stockpile with a calcium sulfate industrial waste. Gypsum, ettringite, and thaumasite were identified as the principal deterioration products. © *1998 Elsevier Science Ltd*

Introduction

A large parking lot developed symptoms of distress, in the form of heaving and rutting soon after its construction. Within a period of 6 months, the magnitude of this problem became severe enough to warrant a thorough investigation as to the cause and extent of this premature distress.

The facility was constructed in an area which is subjected to moisture infiltration because of the flat, low-lying terrain, proximity of the water table (3 to 4 feet), and poorly-drained nature of the subgrade soils. The engineering plans required 6 inches (light duty pavements) of lime-stabilized subgrade (LSS), overlain by 8 inches (heavy duty pavements) of crushed concrete or crushed limestone base, and either a 2-inch (light duty) or 3-inch (heavy duty) hot mix surface layer. Furthermore, the crushed material was required to have a minimum Texas triaxial (1) compressive strength of 45 psi at 0 psi lateral pressure, and 175 psi at 15 psi lateral pressure. These strength levels meet requirements of a Grade 1 (top quality) unbound aggregate base according to Texas Department of Transportation construction specifications. The size gradation of the crushed material was to be tested in accordance with ASTM Method C 136. The liquid limit of the material passing No. 40 sieve was not to exceed 15, and its plasticity index was required to be below 10. The Los Angeles abrasion percent of wear,

[1]To whom correspondence should be addressed.

TABLE 1
Weight loss at specific temperatures.

	Weight Loss (%)			
Sample	55°C	110°C	240°C	LOI
Grey	29.1	4.2	7.0	4.0
White	0.8	4.7	7.0	6.8

tested according to ASTM Method C 131, was to be less than 40. A review of the records revealed that all these specifications were met during the construction of this parking lot.

Nonetheless, at the time the site was inspected by the authors (only 6 months after construction), the base material appeared soft, damp, and friable. Siliceous gravel and limestone fragments, however, were identifiable. The majority of the base had transformed into a material that was distinctly softer than crushed concrete. As a result, loss of density and loss of shear strength had occurred. From visual inspection, massive expansion of the base was evident, as was rutting due to the pressure of slow-moving wheel loads that supported heavy modular structures. In fact, preliminary borehole data of the base indicated varying thickness of 3 to as much as 18 inches.

Experimental

Two sets of samples were collected from the base. The first sample, collected by excavating the base, was grey in color with a relatively high specific gravity. In contrast, the second, which originated from the exposed surface of the base, was white in color, softer, powdery, and much lower in specific gravity.

These samples were thoroughly analyzed using several microanalytical techniques to: 1) identify if crushed concrete had actually been used in the base, and if so, establish the cause of this premature failure of the crushed concrete base, which was designed to last much longer, possibly a few decades; and 2) determine the reaction products, in case there has been a chemical reaction.

Weight loss tests were performed according to ASTM D 2216, and loss on ignition (LOI) was measured in accordance with ASTM C 114 method. Petrographic examination according to ASTM C 856 was carried out to ascertain the presence of crushed concrete in the base; x-ray diffraction (XRD) analysis, differential thermal analysis (DTA), and scanning electron microscopy/energy dispersive X-ray analysis (SEM/EDXA) were used to characterize the original components and reaction products, if any, in the base.

Results

The weight loss results presented in Table 1 illustrate that the bulk of the grey sample remained wet and retained up to 29% moisture, whereas most of the water had evaporated from the white sample. The successive decomposition of constituents at 110 and 240°C suggests that these samples contain at least two families of minerals containing measurable amounts of molecular water. The higher LOI of the white sample indicates the presence of

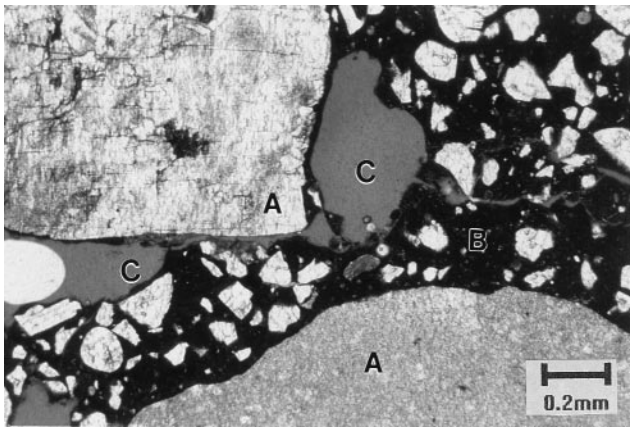

FIG. 1.
Microstructure of reference crushed concrete, collected from site. *A*, aggregate, *B*, paste, *C*, entrapped air void.

more carbonate mineral than was found in the grey sample. This is of some significance and is discussed later.

A fragment of hard material that had washed away from the base was used as the "reference" for petrographic analysis. Thin sections prepared from the reference material and grey and white samples were examined under a polarized transmitted light microscope. Concrete has a characteristic microstructure that is readily recognizable from its petrography. That the reference material is composed of "concrete" was confirmed from the presence of coarse and fine aggregates embedded in a cementitious paste (Fig. 1). Entrapped air voids were also identifiable in the paste. Relict concrete in which both the aggregates and paste have been severely affected was identified in the grey and white samples. The aggregates are mostly siliceous gravel and limestone of local origin. The paste had decomposed, had become extremely porous, and discolored in patches (Fig. 2), while extensive cracks had developed

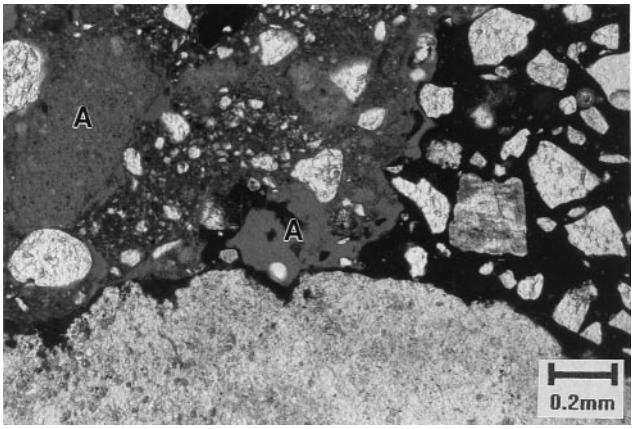

FIG. 2.
Affected concrete with parts having become very porous (*A*).

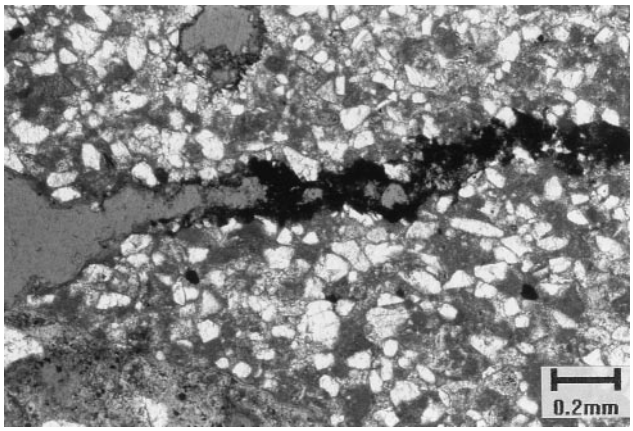

FIG. 3.
Fractured siliceous aggregate in the contaminated crushed concrete base.

in the aggregates (Fig. 3). These deteriorative features are suggestive of chemical attack.

Differential thermal analysis of the grey and white samples was performed under flowing N_2, up to 1000°C. From Figure 4, two groups of sulfate-bearing minerals were detected in these samples. Of these, one constitutes the calcium sulfoaluminate/silicosulfate hydrate or ettringite/thaumasite mineral(s) (2), and the other is gypsum ($CaSO_4 \cdot H_2O$). Owing to the low-temperature loss of lattice-bound water from these minerals, in practice, distinction of analogous minerals, such as ettringite/thaumasite by DTA, is often beyond the resolution of

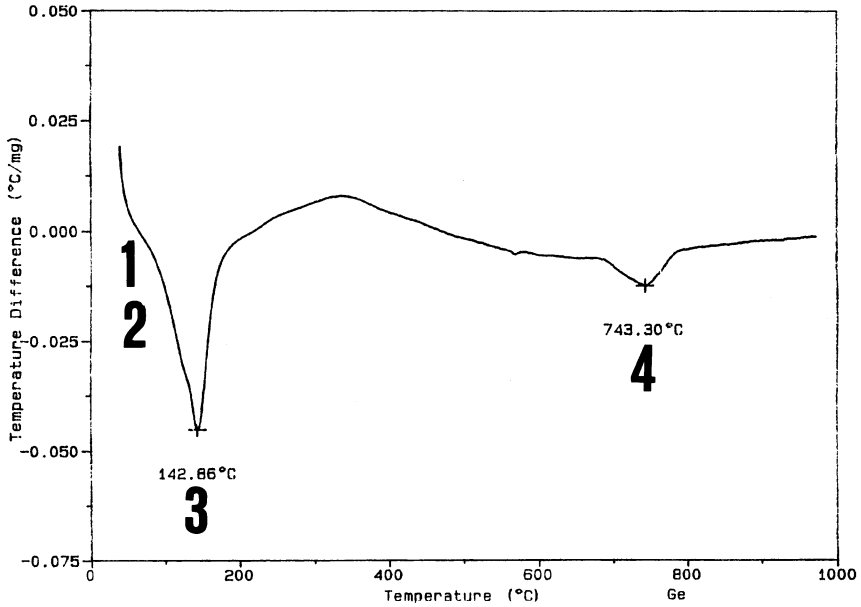

FIG. 4.
DTA of grey sample showing ettringite/thaumasite (*1* and *2*), gypsum (*3*), and calcite (*4*) endotherms.

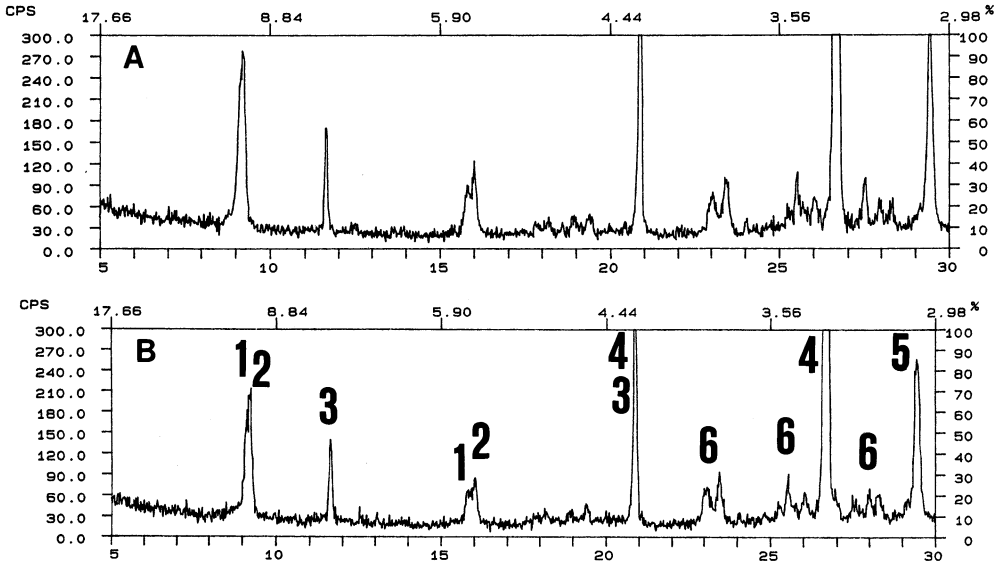

FIG. 5.
XRD patterns of (*a*) grey and (*b*) white samples, where *1* = thaumasite, *2* = ettringite, *3* = gypsum, *4* = quartz, *5* = calcite, and *6* = feldspars.

the instrument. As a matter of fact, a wide range of values are reported for the principal endotherm of thaumasite. These variations are considered to be due to different heating rates used in the analysis and due to the presence of varying amounts of impurities in thaumasite. These minerals only appear as a shoulder on the 140°C endotherm representing gypsum. The other endotherm at 723°C in the DTA plot is characteristic of calcium carbonate decomposition (3).

The XRD analysis revealed the presence of gypsum, calcite ($CaCO_3$), and ettringite, as well as thaumasite (Fig. 5); XRD is the most common method used to detect thaumasite when it is present in large amounts. The thaumasite lines appear at angles slightly higher than the ettringite lines. This effectively means that if both ettringite and thaumasite are present, doublets appear at the "usual" ettringite positions (4). A nominal amount of portlandite, $Ca(OH)_2$, was identified in the grey sample. Additionally, quartz, calcite, and feldspars were found to be present in variable amounts. As the XRDs were performed on as-received samples, no attempt was made to quantify any of the phases. The total absence of either ettringite, thaumasite, or gypsum in the XRD patterns of these samples when heated to 250°C to constant weight (Fig. 6), denotes decomposition of all these hydrate phases, and corroborates with the weight loss results in Table 1.

Careful SEM/EDXA of these samples provided valuable morphological information on the deterioration products and helped to establish the concrete's deterioration mechanism. Lateral expansion along cleavage planes of massive, tabular gypsum crystals (Fig. 7) was evident. A preponderance of ettringite and thaumasite needles and associated cracks were also noted (Fig. 8). Although these minerals are intimately mixed, a clear distinction between the composition of ettringite and thaumasite was possible from EDXA (Fig. 9a and b). No vertical or lateral variations in ettringite/thaumasite proportions, however, could be made. Tiny (<10 μm) crystals of calcite were visible.

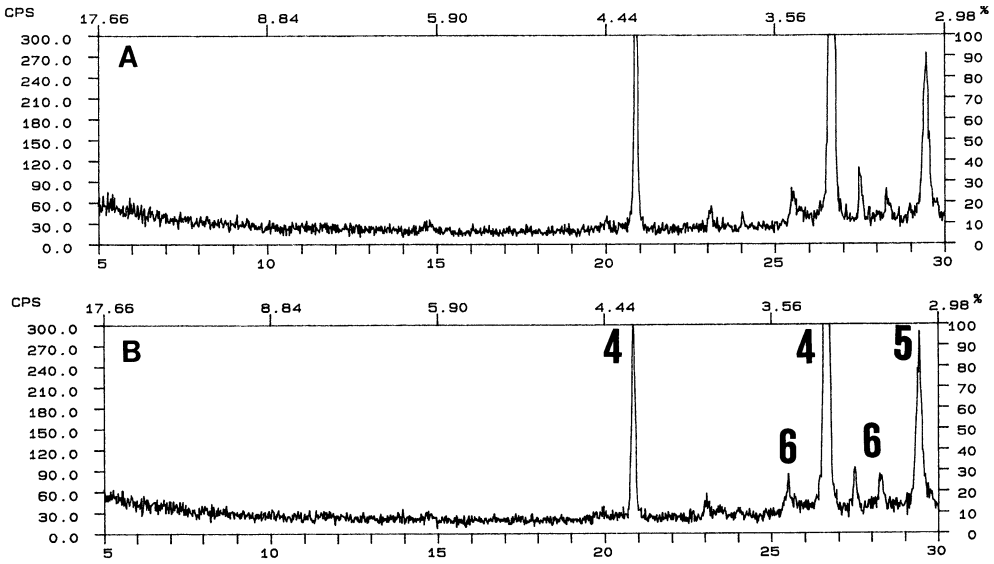

FIG. 6.
XRD patterns of (*a*) grey and (*b*) white samples after heating to 250°C.

The soluble sulfate was analyzed (Table 2) because of the abundance of sulfate-bearing decomposition products in the samples. Analysis of soluble cations was considered unimportant. From this table, it is evident that a high proportion of sulfate ions is in a soluble state and, therefore, quite potent in the sulfate attack of the concrete.

Stabilization of the subgrade soil with 25 pounds per yard (2) of hydrated lime, $Ca(OH)_2$, was specified. Hydrated lime, however, can convert to $CaCO_3$, subject to the availability of adequate moisture and CO_2, the phenomenon being commonly known as carbonation (5).

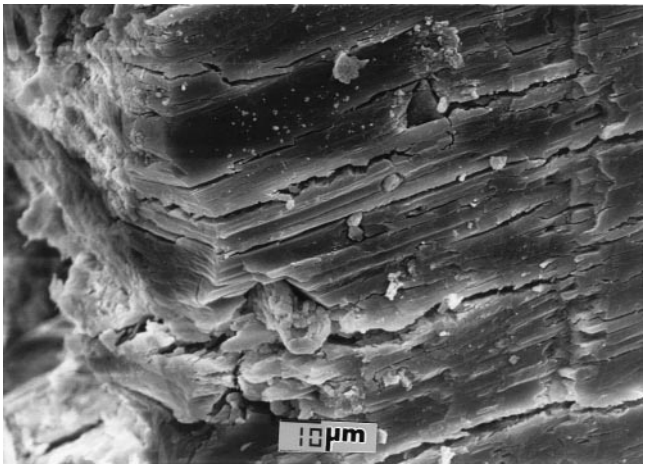

FIG. 7.
Cracks in massive, tabular gypsum crystals.

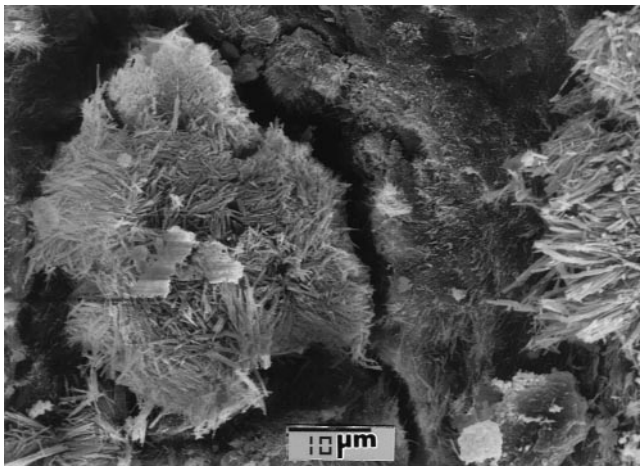

FIG. 8.
Assemblage of ettringite and thaumasite needles and associated cracks.

The soil was identified as silty clay. Two subgrade samples were tested for moisture loss and LOI, with the results listed in Table 3.

Discussion

Petrographic analysis confirmed concrete fragments to be the principal constituent of the base; some of the aggregates could even be traced to their local origin. The grey colored, moist, and decomposed cement paste, upon drying lost weight, appeared lighter in color, and produced a concentration of sulfate ions due to their migration to the surface. This process is comparable to efflorescence (6).

A small amount of $Ca(OH)_2$ in the grey sample as opposed to only $CaCO_3$ in the white, signifies that the former still managed to conserve a marginal amount of concrete constituents.

The presence of substantial amounts of ettringite, thaumasite, and gypsum in cement-based materials is a clear sign of deterioration, although it was not possible to verify if the gypsum detected in the samples was the original contaminant or was the reprecipitated type; the latter being expansive in nature (7). All tests and analyses performed on the white and grey samples indicate severe sulfate attack, which must have occurred through several stages that led to the concrete's total decomposition. According to Mehta (8), it is the $Ca(OH)_2$ and aluminate phases in concrete that are more vulnerable to sulfate attack, resulting in the formation of gypsum and ettringite.

The presence of sulfate and carbonate anions either in the hardened cementitious matrix or in the surrounding medium can initiate thaumasite formation by the transformation of the siliceous components (9,10). Crammond (11) has demonstrated that the breakdown of C-S-H is a key process in the crystallization of thaumasite, whereas the concrete itself can provide the carbonate ions needed. In fact, Regourd (10) posits that all the constituents of concrete can be attacked. Experiments by researchers (12) have shown that thaumasite may either grow on ettringite, or ettringite may convert to thaumasite. Nevertheless, the crystallization

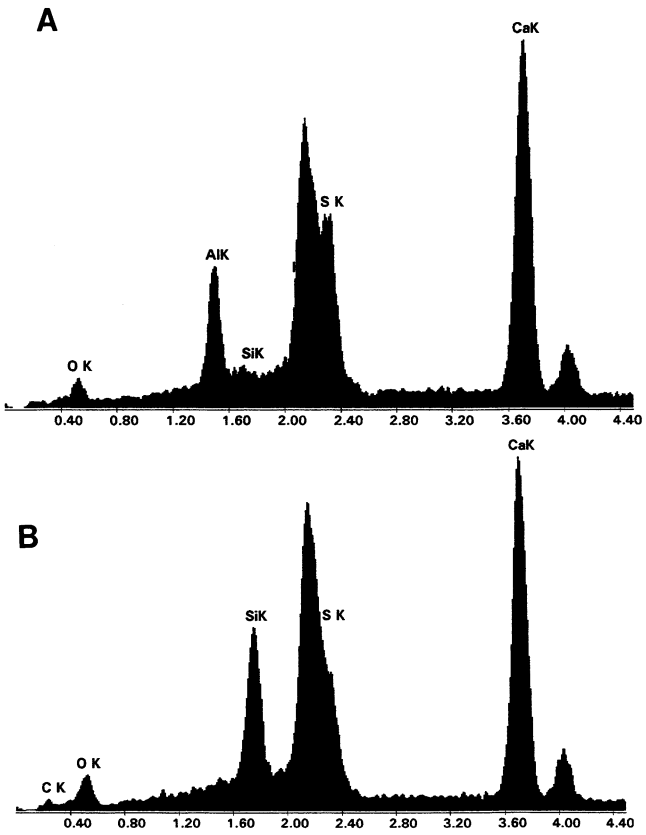

FIG. 9.
EDX spectrum of (*a*) ettringite showing Ca, Al, O, and S peaks, and (*b*) thaumasitee with Ca, Si, O, S and C peaks.

process to a large extent is temperature controlled (13). For example, the formation of ettringite plays a decisive role above 20°C, while at a temperature lower than 10°C it is the formation of thaumasite that plays the determining role.

Although some ettringite can be expected to form in the paste of ordinary Portland cement during its initial hydration, this is considered to be innocuous, whereas secondary ettringite formed later in a mature paste due to sulfate attack or other causes, can create expansion and cracking of the concrete. Thaumasite formation, however, involves the dissolution of the binder phase, which results in softening of the concrete. Berra and Baronio's field studies

TABLE 2
Soluble sulfate analysis results.

Sample	Sulfate (mg/kg)
Laboratory Concrete	89
Grey	2224
White	13470

TABLE 3
Moisture loss and LOI of subgrade.

Sample	Moisture Loss	LOI
1	20.3%	4.3%
2	21.8%	2.6%

(14) showed thaumasite formation from the aggressive action of sulfate and carbonate-bearing ground water in the temperature range of 4 to 6°C. The recorded thermal conditions, the presence of silica, and the free CO_2 in the water were significant enough to warrant the transformation of ettringite to thaumasite.

It is important to consider that the base, after being compacted, was sealed with a 2- to 3-inch asphaltic layer. This sealed unit apparently proved to be an ideal medium for an O_2-deficient or CO_2-rich atmosphere within the base. Following the construction of the base, the site witnessed several cycles of temperature variations ranging from as high as 35° to low as −5°C for a period of nearly 6 months. Additionally, a non-negligible quantity of siliceous gravel and limestone, which happen to be the most common local aggregates, was present in the concrete. This aggregate component later disintegrated under sulfate attack to provide some of the components of the deterioration products. The source of such an enormous amount of sulfate in the base was traced to contamination of the crushed concrete stockpile with a calcium sulfate industrial waste. The authors made no attempt to measure the amount of contaminant, because variations were evident from one location to another, even from visual inspection. Nevertheless, it is not unusual for this lethal combination to have led to the rapid formation of not one, but at least three expansive/destructive forms of minerals: gypsum, secondary ettringite, and thaumasite. The shallow water table may have contributed moisture to the deterioration process by capillary action through the subgrade, but expansion of clay in the soil was positively ruled out as the cause of distress.

Granular $CaCO_3$ observed in the white sample, which is unrelated to the limestone aggregate, may have resulted either from the combination of excess calcium and carbonate in the system following the crystallization of thaumasite, or from carbonation of $Ca(OH)_2$ in the concrete. It is conjectured that the moisture, which already existed in the base, participated in the formation of secondary ettringite. The expansion thus resulted in cracks in the uppermost asphalt layer, which later provided easy channels for migration of water into the base. A significant amount of rain water is considered to have percolated into the base. Further sulfate attack on the siliceous components of the concrete, in a highly carbonated atmosphere in the presence of a substantial amount of moisture, thus caused thaumasite to crystallize.

The moisture content and LOI of the lime-stabilized subgrade, which are still low, indicate that it has still not been affected by the sulfate attack. Nevertheless, the long-term effects of percolation of sulfate ions into the subgrade in such a sulfate-rich medium was not investigated, and therefore, cannot be predicted (15,16).

The structural integrity of the lime-stabilized subgrade was verified in six different location using a dynamic cone penetrometer (DCP). The DCP demonstrated that the lime-stabilized subgrade is about 7 to 10 times stronger than the native subgrade. Trenching in the pavement also revealed a well-stabilized subgrade. The lime-stabilized subgrade has probably significantly reduced the capillary rise potential from the water table into the base layer (17).

Conclusions

An 8-inch-thick crushed concrete base on a 6-inch lime-stabilized subgrade covering a large land area began to develop signs of distress soon after its construction. Within a period of 6 months, heaving and rutting of the base became so severe as to initiate a thorough investigation on the cause of its premature failure.

Severe sulfate attack of the concrete in the base was identified. Preponderant formation of gypsum, ettringite, and thaumasite was noted in the base. As a result of the formation of these minerals, the concrete had become soft, and had expanded. The source of such an abundant supply of sulfate ions was traced to an industrial waste calcium sulfate-contaminated crushed concrete. At the time of investigation, the lime-stabilized subgrade was still in a serviceable condition, and did not indicate any signs of damage.

References

1. Texas Department of Transportation Manual of Testing Procedures, Volume I, Test Method Tex-113E, 1995.
2. W. Lucas, Cem. Concr. Res. 5, 503–518 (1975).
3. S.L. Sarkar, A.K. Bhadra, and P.K. Mandal, Mater. Struct. 27, 548–556 (1994).
4. H.W. Schwander and W.B. Stern, Zement-Kalk-Gips 1, 81–84 (1988).
5. D. Bonen and S.L. Sarkar, Proc. 6th Int. Conf. Cem. Microscopy, Richmond 1–23 (1994).
6. M. Collepardi, Mater. Struct. 23, 81–102 (1990).
7. S.L. Sarkar, Proc. 4th CANMET/ACI Int. Conf. Durability of Concr., Sydney 1357–1378 (1997).
8. P.K. Mehta, Concrete Structure, Properties, and Materials, Prentice Hall, Inc., Englewood Cliffs, 1986.
9. G. Leifeld et al., Zement-Kalk-Gips 1, 174–177 (1970).
10. M. Regourd et al., ASTM STP 691, P.J. Sereda and G.G. Litvan (eds.), pp. 254–268, 1980.
11. N.J. Crammond, Durability of Building Materials and Components, Vol. 1, S. Nagataki et al. (eds.), pp. 295–305, E&FN SPON, London, 1991.
12. U. Ludwig and S. Mehr, Proc. 8th Int. Congr. Chem. Cem., Rio de Janeiro, 5, 181–188 (1986).
13. F.F. Alksnis and V.I. Alksne, Proc. 8th Int. Congr. Chem. Cem., Rio de Janeiro, 5, 170–174 (1986).
14. M. Berra and G. Baronio, ACI SP 100, 2, 2073–2089 (1987).
15. T.M. Petry and D.N. Little, Evaluation of Problematic Sulfate Levels Causing Sulfate Induced Heave in Lime-Stabilized Clay Soils, Transportation Research Board, 1993.
16. D.N. Little and T.M. Petry, Recent Developments in Sulfate-induced Heave in Treated Expansive Clays, Second Interagency Symposium on Stabilization of Soils and Other Materials, Metarie, LA, 1992.
17. D.N. Little, Stabilization of Pavement Subgrades and Base Courses with Lime, Kendall/Hunt Publishing Co., Dubuque, 1995.